Accepted Manuscript

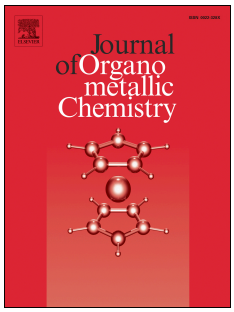

Synthesis and characterization of chiral phosphirane derivatives of [(μ-H)$_4$Ru$_4$(CO)$_{12}$] and their application in the hydrogenation of an α,β-unsaturated carboxylic acid

Ahmed F. Abdel-Magied, Maitham H. Majeed, Manuel F. Abelairas-Edesa, Arne Ficks, Radwa M. Ashour, Ahibur Rahaman, William Clegg, Matti Haukka, Lee J. Higham, Ebbe Nordlander

PII: S0022-328X(17)30327-3

DOI: 10.1016/j.jorganchem.2017.05.031

Reference: JOM 19957

To appear in: *Journal of Organometallic Chemistry*

Received Date: 10 February 2017

Revised Date: 12 May 2017

Accepted Date: 15 May 2017

Please cite this article as: A.F. Abdel-Magied, M.H. Majeed, M.F. Abelairas-Edesa, A. Ficks, R.M. Ashour, A. Rahaman, W. Clegg, M. Haukka, L.J. Higham, E. Nordlander, Synthesis and characterization of chiral phosphirane derivatives of [(μ-H)$_4$Ru$_4$(CO)$_{12}$] and their application in the hydrogenation of an α,β-unsaturated carboxylic acid, *Journal of Organometallic Chemistry* (2017), doi: 10.1016/j.jorganchem.2017.05.031.

Tetraruthenium tetrahydrido clusters containing chiral binaphthyl-derived mono- or di-phosphiranes have been synthesized and characterized. The phosphirane-substituted clusters were found to be good catalysts for the hydrogenation of tiglic acid (*trans*-2-methyl-2-butenoic acid) but enantioselective hydrogenation could not be detected.

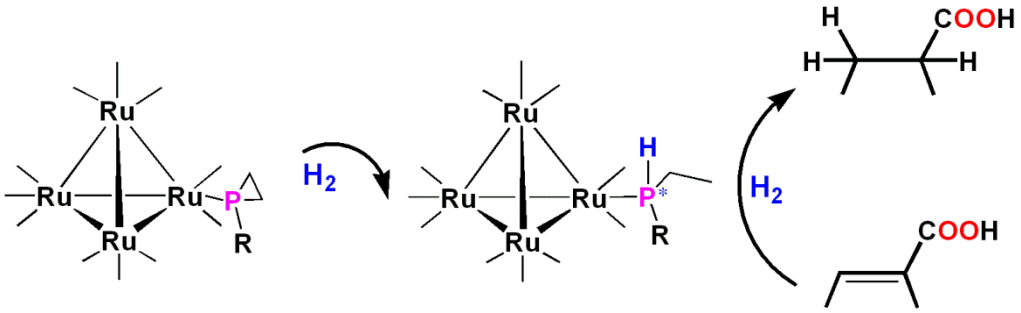

Synthesis and characterization of chiral phosphirane derivatives of $[(\mu\text{-H})_4Ru_4(CO)_{12}]$ and their application in the hydrogenation of an α,β-unsaturated carboxylic acid

Ahmed F. Abdel-Magied,[a] Maitham H. Majeed,[a] Manuel F. Abelairas-Edesa,[b] Arne Ficks,[b] Radwa M. Ashour,[a] Ahibur Rahaman,[a] William Clegg,[b] Matti Haukka,[c] Lee J. Higham[b]* and Ebbe Nordlander[a]*

[a] Inorganic Chemistry Research Group, Chemical Physics, Chemical Center, Lund University, Box 124, SE-221 00, Lund, Sweden.
[b] School of Chemistry, Bedson Building, Newcastle University, Newcastle upon Tyne, NE1 7RU, U.K.
[c] Department of Chemistry, University of Jyväskylä, P.O. Box 35, FI-40014 Jyväskylä, Finland.

Dedicated to Prof. Richard D. Adams on his 70th birthday, and in recognition of his outstanding contributions to organometallic cluster chemistry.

ABSTRACT:

Ruthenium clusters containing the chiral binaphthyl-derived mono-phosphiranes [(*S*)-([1,1′-binaphthalen]-2-yl)phosphirane] (*S*)-**1a**, [(*R*)-(2′-methoxy-1,1′-binaphthyl-2-yl)phosphirane] (*R*)-**1b**, and the diphosphirane [2,2′-di(phosphiran-1-yl)-1,1′-binaphthalene] (*S*)-**1c** have been synthesized and characterized. The clusters are $[(\mu\text{-H})_4Ru_4(CO)_{11}$((*S*)-**1a**)] (*S*)-**2**, $[(\mu\text{-H})_4Ru_4(CO)_{11}$((*R*)-**1b**)] (*R*)-**3**, 1,1-$[(\mu\text{-H})_4Ru_4(CO)_{10}$((*S*)-**1c**)] (*S*)-**4**, $[(\mu\text{-H})_4Ru_4(CO)_{11}$((*S*)-binaphthyl-$P_{(s)}$(H)Et)] ($S,S_p$)-**5**, $[(\mu\text{-H})_4Ru_4(CO)_{11}$((*S*)-binaphthyl-$P_{(R)}$(H)Et)] ($S,R_p$)-**6**, $[(\mu\text{-H})_4Ru_4(CO)_{11}$((*R*)-binaphthyl-$P_{(s)}$(H)Et)] ($R,S_p$)-**7**, $[(\mu\text{-H})_4Ru_4(CO)_{11}$((*R*)-binaphthyl-$P_{(R)}$(H)Et)] ($R,R_p$)-**8** and the phosphinidene-capped triruthenium cluster $[(\mu\text{-H})_2Ru_3(CO)_9(PEt)]$ **9**. Clusters **5-8** are formed via hydrogenation and opening of the phosphirane ring in clusters (*S*)-**2** and (*R*)-**3**. The phosphirane-substituted clusters were found to be able to catalyze the hydrogenation of *trans*-2-methyl-2-butenoic acid (tiglic acid), but no enantioselectivity could be detected. The molecular structures of (*S*)-**4**, (R,S_p)-**7** and **9** have been determined and are presented.

KEYWORDS: Hydrogenation, Clusters, Ruthenium, Phosphirane

1. Introduction

For more than three decades, numerous researchers in both academia and industry have investigated the homogeneous asymmetric hydrogenation reaction extensively, due to its importance for the production of enantiopure bioactive ingredients on an industrial scale [1]. Ruthenium, rhodium and iridium complexes containing chiral diphosphine ligands have shown high catalytic activity in the asymmetric hydrogenation of alkenes, ketones and imines [2, 3]. There has also been considerable interest in the synthesis and use of transition metal carbonyl clusters as catalysts for various chemical reactions of industrial relevance [4-8]. Previously, cluster-based catalysts/catalyst precursors have shown interesting catalytic activity for several different chemical reactions: hydride-containing trinuclear and tetranuclear ruthenium carbonyl clusters have been used effectively in a number of reactions including isomerizations [9], hydroformylations [10], hydrosilylations [11], reductive couplings [12] and the water-gas shift reaction [13]. Relatively few studies have dealt with the potential of clusters to act as catalysts for the asymmetric hydrogenation of carboxylic acids [14-17]. Salvini *et al*. have reported the application of such clusters in the asymmetric hydrogenation of tiglic acid (*trans*-2-methyl-2-butenoic acid) [18], but the reaction was performed under rather harsh conditions and the formation of 2-methylbutyric acid was obtained with relatively low enantioselectivities (6-39% *ee*). Catalyst activities and selectivities were found to be dependent on the chiral phosphine ligands coordinated to the parent cluster. Using relatively bulky, chiral diphosphine ligands with ferrocenyl backbones (the Walphos and Josiphos ligand families), we have shown that tetraruthenium tetrahydride clusters can be effective catalysts/catalyst precursors under mild hydrogenation conditions for the asymmetric hydrogenation of α-unsaturated carboxylic acids, with enantioselectivities exceeding 90% *ee* in certain cases [19-22].

The common monodentate binaphthyl-based ligands with phosphonite [23], phosphite [24] and phosphoramidite [25] functionalities have also received attention as ligands in asymmetric hydrogenation reactions. Few examples are known where chiral phosphiranes were synthesized and used in asymmetric catalysis; phosphiranes are highly strained heterocycles that incorporate the phosphorus atom into a three-membered ring, and as a result of their highly pyramidalised structure, are considered weak σ-donors but strong π-acceptors [26]. Rhodium complexes of phosphiranes

have been used in the asymmetric α–dehydroamination of acids and itaconates, achieving enantioselectivities of up to 76% *ee* [27], whilst Higham and co-workers have shown that binaphthyl-derived phosphiranes can be used effectively in the asymmetric hydrosilylation of styrene, with 100% conversion and 80% *ee*. The asymmetric allylic alkylation of (*rac*)-(*E*)-1,3-diphenylallyl acetate was achieved with the same phosphirane ligands, giving high conversions of up to 91%, albeit with relatively low *ee* values of around 17% [28, 29].

Considering the success of our earlier studies, and the demonstrated effectiveness of binaphthyl-based phosphorus-donor ligands, we have investigated the coordination of chiral phosphiranes to H_4Ru_4 carbonyl clusters, and the potential of the resultant chiral ruthenium clusters to catalyze asymmetric reactions. Herein, we report the synthesis and characterization of new tetranuclear ruthenium clusters containing the chiral mono- or bidentate phosphirane ligands [(*S*)-([1,1′-binaphthalen]-2-yl)phosphirane] (*S*)-**1a**, [(*R*)-(2′-methoxy-1,1′-binaphthyl-2-yl)phosphirane] (*R*)-**1b**, and [2,2′-di(phosphiran-1-yl)-1,1′-binaphthalene] (*S*)-**1c** (Figure 1). A comparison of their performances as catalysts/catalyst precursors in the hydrogenation of tiglic acid is also provided.

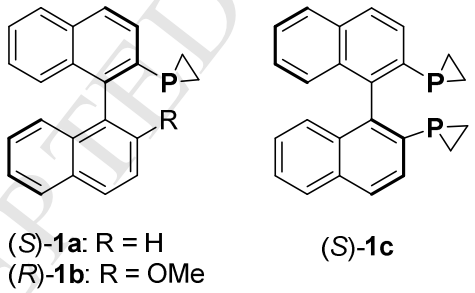

Figure 1. The structures of the phosphirane ligands used in this investigation.

2. Results and discussion

The syntheses of the chiral MOP-type ([1,1′-binaphthalen]-2-yldiphenylphosphine) derivatives of $[H_4Ru_4(CO)_{12}]$ were based on previously published methods [19, 21, 22], i.e. *via* thermal substitution in benzene under an elevated pressure of hydrogen gas (30-50 bar), or by using Me_3NO as an oxidative decarbonylation reagent in the presence of the phosphirane ligand in dichloromethane solution, at ambient

temperature (*cf*. Experimental Section). The latter method was found to be superior with respect to both yield and selectivity of product formation, while the thermal high-pressure route gave rise to phosphirane degradation (*vide infra*). The clusters were identified by IR, ^{1}H and ^{31}P NMR spectroscopy, mass spectrometry and, wherever possible, X-ray crystallography. A summary of the new clusters synthesized in this study is given in Table 1.

Table 1. A summary of the cluster framework geometries and phosphirane coordination modes detected in this study.

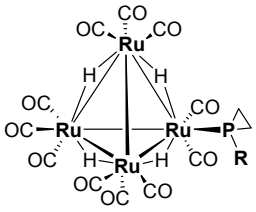

$[(\mu\text{-H})_4Ru_4(CO)_{11}((S)\text{-}\mathbf{1a})]$ (*S*)-**2**
$[(\mu\text{-H})_4Ru_4(CO)_{11}((R)\text{-}\mathbf{1b})]$ (*R*)-**3**

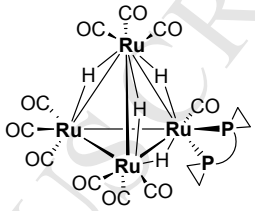

1,1-$[(\mu\text{-H})_4Ru_4(CO)_{10}((S)\text{-}\mathbf{1c})]$ (*S*)-**4**

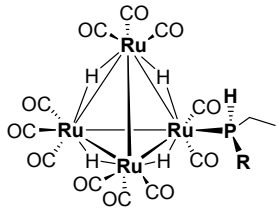

$[(\mu\text{-H})_4Ru_4(CO)_{11}((S)\text{-H-binaphthyl-P}_{(S)}(H)Et)]$ (*S,Sp*)-**5**
$[(\mu\text{-H})_4Ru_4(CO)_{11}((R)\text{-MeO-binaphthyl-P}_{(S)}(H)Et)]$ (*R,Sp*)-**7**

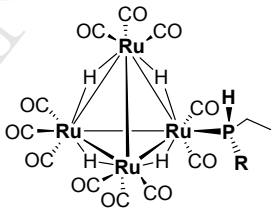

$[(\mu\text{-H})_4Ru_4(CO)_{11}((S)\text{-H-binaphthyl-P}_{(R)}(H)Et)]$ (*S,Rp*)-**6**
$[(\mu\text{-H})_4Ru_4(CO)_{11}((R)\text{-MeO-binaphthyl-P}_{(R)}(H)Et)]$ (*R,Rp*)-**8**

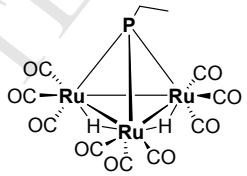

$[(\mu\text{-H})_2Ru_3(CO)_9(PEt)]$ **9**

2.1. Synthesis and characterization of clusters (S)-2, (R)-3 and (S)-4

Treatment of an equimolar mixture of $[H_4Ru_4(CO)_{12}]$ and (*S*)-**1a**, (*R*)-**1b** or (*S*)-**1c** in dichloromethane at room temperature with 1.2-1.5 eq. of the oxidative decarbonylation reagent Me_3NO led to the formation of the corresponding monosubstituted clusters $[(\mu\text{-H})_4Ru_4(CO)_{11}((S)\text{-}\mathbf{1a})]$ (*S*)-**2**, $[(\mu\text{-H})_4Ru_4(CO)_{11}((R)\text{-}\mathbf{1b})]$ (*R*)-**3**, or the chelated diphosphirane cluster 1,1-$[(\mu\text{-H})_4Ru_4(CO)_{10}((S)\text{-}\mathbf{1c})]$ (*S*)-**4**. Purification by preparative thin-layer chromatography allowed for the isolation of each cluster as an orange-red solid. The structures of the clusters were identified on

the basis of their spectroscopic data. The IR spectra of (*S*)-**2** and (*R*)-**3** are similar to those previously reported for the clusters $[(\mu\text{-H})_4Ru_4(CO)_{11}(L)]$ (L = PMe_2Ph) [30] and $[(\mu\text{-H})_4Ru_4(CO)_{11}(NMDPP)]$ (NMDPP = (*S*)-(+)-neomenthyldiphenylphosphine] [20]. The ^1H NMR spectra revealed, in addition to the signals for the chiral phosphirane ligands (*cf.* Experimental section), an apparent doublet at –17.64 ppm for (*S*)-**2** (J_{HH} = 4.6 Hz) and an apparent singlet at –17.84 ppm for (*R*)-**3**, which indicates a complete fluxionality of the hydride ligands (*vide infra*). The ^{31}P NMR spectra show a broad multiplet at –154.2 ppm for (*S*)-**2** and an apparent singlet at –155.9 ppm for (*R*)-**3**, in contrast to the high field shifts shown by the free ligands themselves ($^{31}P[^1H]$ NMR: (*S*)-**1a** –235.4 ppm, (*R*)-**1b** –235.0 ppm) [28]. The mass spectra reveal peak envelopes at *m*/*z* = 1052 $[M+Na]^+$ and 1081 $[M+Na]^+$ which correspond to the molecular formulae $[(\mu\text{-H})_4Ru_4(CO)_{11}((S)\text{-}\mathbf{1a})]$ (*S*)-**2** and $[(\mu\text{-H})_4Ru_4(CO)_{11}((R)\text{-}\mathbf{1b})]$ (*R*)-**3**, respectively.

The IR spectrum of cluster (*S*)-**4** in cyclohexane exhibits eight absorptions in the CO region. The $\nu_{C\text{-}O}$ IR stretching frequency pattern of (*S*)-**4** is thus in agreement with that of the known complex 1,1-$[(\mu\text{-H})_4Ru_4(CO)_{10}(DUPHOS)]$ [DUPHOS = (2*R*,5*R*)-2,5-dimethyl-1-(2-((2*R*,5*R*)-2,5-dimethylphospholan-1-yl)-phenyl)phospholane] [20], which indicates that the diphosphirane ligand (*S*)-**1c** in cluster (*S*)-**4** chelates one ruthenium apex. The ^1H and ^{31}P NMR spectra of (S)-**4** show one broad singlet at –17.20 ppm in the hydride region of the ^1H NMR spectrum (due to hydride fluxionality), while the ^{31}P NMR spectrum displays two doublets ($J_{P\text{-}P}$ = 37.1 Hz) with equal intensity at –135.6 and –139.2 ppm caused by the two magnetically inequivalent phosphorus nuclei. The mass spectrum of (*S*)-**4** reveals a peak at *m*/*z* = 1082 $[M+Na]^+$, which is consistent with the molecular formula $[(\mu\text{-H})_4Ru_4(CO)_{10}((S)\text{-}\mathbf{1c})]$ (*S*)-**4**.

It was possible to grow crystals of (*S*)-**4** suitable for analysis by X-ray diffraction. The chelating mode of the diphosphirane ligand could therefore be unambiguously confirmed in the solid state. The molecular structure of (*S*)-**4** is shown in Figure 2. The cluster contains a distorted tetrahedral core of ruthenium atoms with the 'basal' atoms preserving the tricarbonyl units of the parent cluster $[H_4Ru_4(CO)_{12}]$ [31]. The diphosphirane ligand is coordinated to the 'apical' atom, Ru1, in a chelating binding mode. The Ru-Ru bond lengths provide a good indication of the locations of the hydrides. They may be divided into two distinctive classes: firstly the four 'long'

(hydride-bridged) distances [Ru1-Ru2 2.9795(4), Ru1-Ru3 3.0055(4), Ru1-Ru4 2.9518(4), Ru2-Ru3 2.9229(4)Å], and secondly the two 'short' distances [Ru3-Ru4 2.7919(4), Ru2-Ru4 2.7945(4)Å]. The arrangement of the four bridging hydrides yields an H_4Ru_4 cluster-core with C_s symmetry, rather than the D_{2d} symmetry that was observed for the bis-phosphine-derivatised cluster $[H_4Ru_4(CO)_{10}(PPh_3)_2]$ [31]. The C_s symmetry found in the H_4Ru_4 core seems to be a common feature that is shared with $[H_4Ru_4(CO)_{10}$(diphosphine)] clusters, and has been reported for both chelating [19] and bridging [19, 22] coordination modes of the diphosphine ligands. The Ru-P distances in cluster (*S*)-**4** are identical within experimental error: [Ru1-P1 2.3017(3), Ru1-P2 2.3019 (3)Å]. All CO ligands are bound in a terminal monodentate coordination mode and are staggered with respect to the Ru-Ru vectors. It should be noted that due to the chirality of the binaphthyl backbone, the two phosphorus atoms of the bound ligand are magnetically inequivalent, regardless of hydride fluxionality. The high degree of hydride fluxionality that was exhibited for (*S*)-**2**, (*R*)-**3** and (*S*)-**4** at ambient temperature is in contrast to what was found for related (chiral) phosphine derivatives of H_4Ru_4 [21, 22]. Attempts to freeze-out the fluxionality in (*S*)-**2** and (*S*)-**4** by means of low temperature ^{1}H NMR experiments were unsuccessful; the fluxional behaviour was observed even at 213 K (*cf*. ESI†).

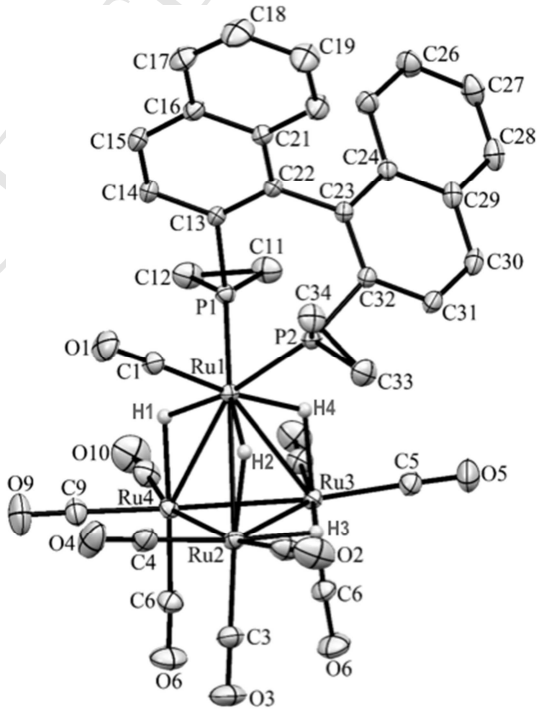

Figure 2. Molecular structure of 1,1-[(μ-H)$_4$Ru$_4$(CO)$_{10}$((*S*)-**1c**)] (*S*)-**4** with thermal ellipsoids drawn at the 50% probability level. All hydrogen atoms except the hydrides have been omitted for clarity. Selected bond lengths (Å): Ru1-Ru2 2.9795(4), Ru1-Ru3 3.0055(4), Ru1-Ru4 2.9518(4), Ru2-Ru3 2.9229(4), Ru3-Ru4 2.7919(4), Ru2-Ru4 2.7945(4), Ru1-P1 2.3017(3), Ru1-P2 2.3019(3).

*2.2. Synthesis and characterization of clusters (S,S$_P$)-**5**, (S,R$_P$)-**6**, (R,S$_P$)-**7** and (R,R$_P$)-**8***

The reaction of [(μ-H)$_4$Ru$_4$(CO)$_{12}$] with an equimolar amount of (*S*)-**1a** or (*R*)-**1b** under elevated temperature and H_2 pressure (30-50 bar, *cf*. Experimental Section) led to degradation of the phosphirane ligands. Cleavage of a P-C bond in the strained three-membered phosphirane ring occurred, and hydrogenation gave the resultant binaphthylPH(Et) secondary phosphine moiety, thus introducing another element of chirality into each ligand. As a result, the diastereomeric pairs [(μ-H)$_4$Ru$_4$(CO)$_{11}$((*S*)-binaphthyl-P$_{(s)}$(H)Et)] (*S*,*S*$_P$)-**5** and [(μ-H)$_4$Ru$_4$(CO)$_{11}$((*S*)-binaphthyl-P$_{(R)}$(H)Et)] (*S*,*R*$_P$)-**6**, or [(μ-H)$_4$Ru$_4$(CO)$_{11}$((*R*)-binaphthyl-P$_{(s)}$(H)Et)] (*R*,*S*$_P$)-**7** and [(μ-H)$_4$Ru$_4$(CO)$_{11}$((*R*)-binaphthyl-P$_{(R)}$(H)Et)] (*R*,*R*$_P$)-**8** were formed, comprising opposite stereocenters at the phosphorus atom of each pair.

Whether the ligand transformation occurs before or after coordination to the tetraruthenium clusters was initially unclear. However, it was subsequently found that the same diastereomeric pairs could be formed via direct thermolysis of [(μ-H)$_4$Ru$_4$(CO)$_{11}$((*S*)-**1a**)] (*S*)-**2** or [(μ-H)$_4$Ru$_4$(CO)$_{11}$((*R*)-**1b**)] (*R*)-**3** under high H_2 pressure (*cf*. Scheme 1 and Experimental Section). When ligand (*S*)-**1a** was heated under the same reaction conditions, but in the absence of [(μ-H)$_4$Ru$_4$(CO)$_{12}$], no hydrogenation or degradation of the ligand was observed. This strongly indicates that the hydrogenation of the ligand is mediated by the ruthenium cluster.

The clusters were isolated by preparative thin-layer chromatography as red-orange solids. The spectroscopic data were found to be consistent with the proposed structures discussed above, which are depicted in Scheme 1. The $\nu_{C\text{-}O}$ IR patterns of (*S*,*S*$_P$)-**5**/(*S*,*R*$_P$)-**6** and (*R*,*S*$_P$)-**7**/(*R*,*R*$_P$)-**8** are in agreement with those reported for mono-substituted [(μ-H)$_4$Ru$_4$(CO)$_{11}$(L)] clusters, *e.g*. where L = PMe$_2$Ph [30] or NMDPP ((*S*)-(+)-neomenthyldiphenylphosphine) [20]. The ^{1}H NMR spectra revealed, in addition to signals for the chiral secondary phosphine ligand, apparent singlets at –17.64 ((*S*,*S*$_P$)-**5**), –17.81 ((*S*,*R*$_P$)-**6**), –17.72 ((*R*,*S*$_P$)-**7**) and –17.86 ppm ((*R*,*R*$_P$)-**8**), due

to the high degree of hydride fluxionality in each cluster at ambient temperature. Variable-temperature ^{1}H NMR of clusters (S,S_P)-**5** and (S,R_P)-**6** showed that the fluxionality remained even at 213K (*vide supra*, *cf.* Supplementary Information). Furthermore, the ^{1}H NMR spectra confirmed the opening of the three-membered phosphorus-heterocycle of the phosphirane ligands, which is highly strained as a result of the small bond angle at the phosphorus atom [32]. In all four clusters the ^{1}H NMR resonances of the ethyl group were observed, as well as the signal for the hydrogen atom coordinated directly to the phosphorus. The latter resonance appeared as a doublet at 5.23 ppm for (S,S_P)-**5** ($^1J_{H\text{-}P}$ = 381 Hz), 5.28 ppm for (S,R_P)-**6** ($^1J_{H\text{-}P}$ = 379 Hz) 5.16 ppm for (R,S_P)-**7** ($^1J_{H\text{-}P}$ = 380 Hz) and 5.22 ppm for (S,S_P)-**8** ($^1J_{H\text{-}P}$ = 378 Hz). The ^{31}P NMR spectra for clusters (S,S_P)-**5**/(S,R_P)-**6** and (R,S_P)-**7**/(R,R_P)-**8** show signals that are shifted to lower field at –11.9, –13.1, –11.8 and –13.2 ppm, respectively (partial ^{1}H decoupling, *cf.* Supplementary Material). The mass spectra revealed peak envelopes at m/z = 1035 $[M+H]^+$ for (S,S_P)-**5**/(S,R_P)-**6** and 1083 $[M+Na]^+$ for (R,S_P)-**7**/(R,R_P)-**8**, in agreement with the proposed molecular formulae.

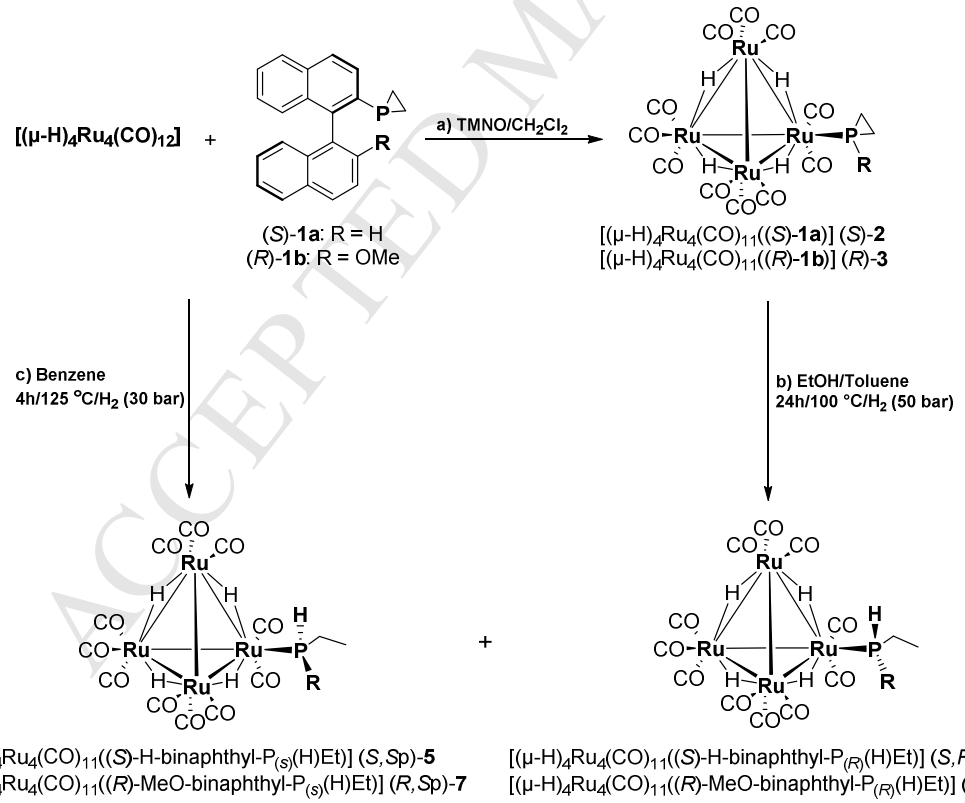

Scheme 1. Synthesis of clusters (*S*)-**2**, (*R*)-**3**, (S,S_P)-**5**, (S,R_P)-**6**, (R,S_P)-**7** and (R,R_P)-**8**.

The nature of the transformed phosphirane ligand was unambiguously confirmed by the determination of the solid-state structure of (*R*,*S*$_P$)-**7**, shown in Figure 3. Relevant bond distances are summarized in the figure caption, and crystallographic data are collated in Table S1. The symmetry of the $Ru_4(\mu\text{-}H)_4$ core is D_{2d}, which is in agreement with previously reported crystal structures of other $[H_4Ru_4(CO)_{11}(PR_3)]$ species (R = OMe [30], Ph [33], SC_4H_3 [34], C_6F_5 [30], OEt [30]) and the diphosphine bridged cluster $[\{H_4Ru_4(CO)_{11}\}_2(\mu\text{-}Ph_2\text{-}P\text{-}C{\equiv}C\text{-}C{\equiv}C\text{-}PPh_2)]$ [35]. The one exception, with C_s symmetry, was reported for $[H_4Ru_4(CO)_{11}(NMDPP)]$ (NMDPP = (S)-(+)-neomenthyldiphenylphosphine) [20]. The *trans* P1-Ru4-Ru2 bond angle (*cf*. Figure 3) is close to linear at 170.124(18)° and comparable to the value found in $[H_4Ru_4(CO)_{11}\{P(C_6F_5)_3\}]$ of 172.25(3)°.

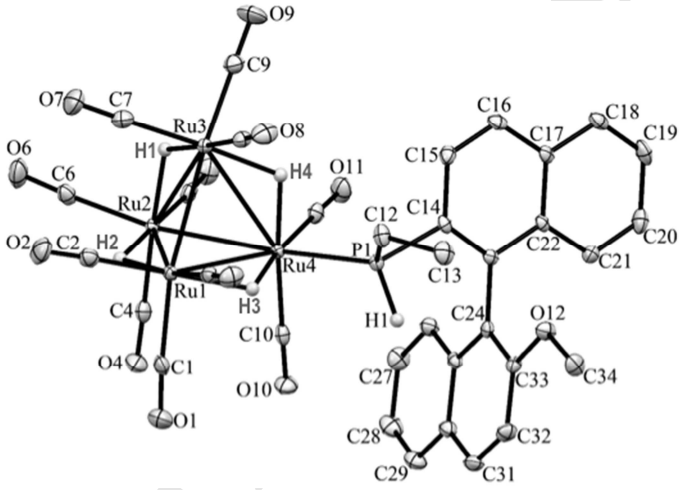

Figure 3. Molecular structure of $[(\mu\text{-}H)_4Ru_4(CO)_{11}((R)\text{-binaphthyl-}P_{(s)}(H)Et)]$ (*R*,*S*$_P$)-**7** with thermal ellipsoids drawn at 50% probability level. Aryl hydrogen atoms have been omitted for clarity. Selected bond lengths (Å): Ru1-Ru2 2.9627(3), Ru1-Ru3 2.7891(3), Ru1-Ru4 2.9615(3), Ru2-Ru3 2.9584(3), Ru3-Ru4 2.3274(6), Ru2-Ru4 2.7863(3), Ru4-P1 2.3274(6).

Following on from this, it was envisaged that the formation of phosphido clusters via CO dissociation and oxidative addition of a P-H bond at a ruthenium center may be possible, considering that the four clusters (*S*,*S*$_P$)-**5**/(*S*,*R*$_P$)-**6** and (*R*,*S*$_P$)-**7**/(*R*,*R*$_P$)-**8** each contain a secondary phosphine. Therefore, attempts were made to promote such a transformation by either (*i*) dissolving the aforementioned secondary phosphine cluster species in THF followed by the addition of Me_3NO in THF under nitrogen and subsequently refluxing the solution for 12 h, or (*ii*) refluxing in toluene for 5h.

However, thin-layer-chromatographic analysis indicated that in all cases no reaction had occurred.

However, it was found that thermolysis of [(μ-H)$_4$Ru$_4$(CO)$_{11}$((*S*)-binaphthyl-P$_{(s)}$(H)Et)] (*S*,*S*$_P$)-**5** in benzene under 50 bar of H_2, for 24 h at a temperature of 100 ºC, led to the formation of a small amount of *phosphinidene* clusters. One product was identified as [(μ-H)$_2$Ru$_3$(CO)$_9$(μ$_3$-(*S*)-binaphthyl-P)] on the basis of its ^{1}H and ^{31}P NMR spectra [36]. A second product was recrystallized from acetonitrile-hexane solution, where a few red crystals were formed, which when analyzed by single crystal X-ray diffraction (*vide infra*) were identified as [(μ-H)$_2$Ru$_3$(CO)$_9${μ$_3$-P(C$_2$H$_5$)}] **9**. These phosphinidene clusters are presumably formed via opening/hydrogenation of the phosphirane moiety, together with (subsequent) elimination of either the ethyl or the binaphthyl moiety. Because of the very poor yield, no spectroscopic data for compound **9** are available (further attempts to resynthesize compound **9** have failed).

The solid-state structure of **9** is shown in Figure 4, with selected geometric data listed in the caption; relevant crystallographic data are summarized in Table S1. In **9**, the three ruthenium atoms are capped by the phosphorus atom, forming a distorted tetrahedral core. The distortion originates from the edge-bridging hydrides that link Ru1-Ru2 and Ru1-Ru3. Due to the influence exerted by the edge-bridging hydrides, the Ru1-Ru2 and Ru1-Ru3 bond distances (2.9392(2) and 2.9413(3)Å, respectively) are elongated relative to the Ru2-Ru3 bond distance (2.8225(2)Å). The Ru-P bond distances are similar to those observed for the phosphinidene cluster [H$_2$Ru$_3$(CO)$_9$(PPh)] [37]. However, in **9**, the Ru-P bond lengths are notably asymmetric: Ru1-P1 = 2.3253(6), Ru2-P1 = 2.2840(6) and Ru3-P1 = 2.2907(6)Å.

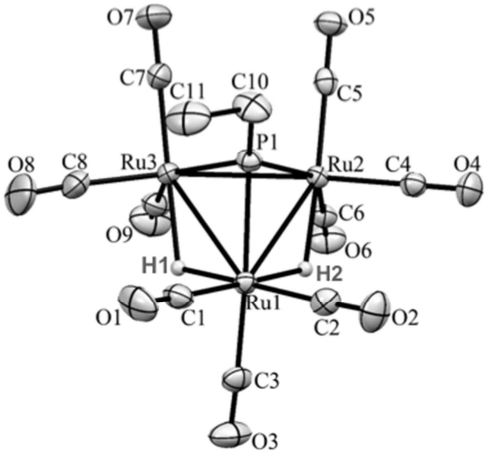

Figure 4. Molecular structure of [(μ-H)$_2$Ru$_3$(CO)$_9$(PEt)] **9** with thermal ellipsoids drawn at 50% probability level. All hydrogen atoms except the hydrides have been omitted for clarity. Selected bond lengths (Å): Ru1-Ru2 2.9392(2), Ru1-Ru3 2.9413(3), Ru2-Ru3 2.8225(2), Ru1-P1 2.3253(6), Ru2-P1 2.2840(6), Ru3-P1 2.2907(6).

2.3. Hydrogenation of tiglic acid

For the asymmetric hydrogenation of tiglic acid ((*E*)-2-methylbut-2-enoic acid) catalyzed by H_4Ru_4-clusters, we have shown repeatedly that at the comparatively low temperature of 100 °C and with a hydrogen pressure of 50 bar, the reaction conversion is maximized and the selectivity is enhanced [21, 22]. At higher temperatures (130-150 °C), severe decomposition of the clusters was observed and it is suspected that the solid particles produced in the reaction mixture were responsible for the formation of a considerable amount of cyclohexene and cyclohexane, in addition to the expected 2-methyl butyric acid [20]. However, at 100 °C the reaction mixture remained homogeneous and the aforementioned hydrogenation products, derived from toluene, were not detected although longer reaction times of up to 48 h were required in order to increase the conversion. The results of the catalytic tests using clusters (*S*)-**4**, (*S,S*$_P$)-**5**, (*S,R*$_P$)-**6**, (*R,S*$_P$)-**7** and (*R,R*$_P$)-**8** are presented in Table 2. Clusters (*S*)-**2** and (*R*)-**3** were not included in the study, because under the catalytic reaction conditions described in Scheme 1, they generated (*S,S*$_P$)-**5**/(*S,R*$_P$)-**6** and (*R,S*$_P$)-**7**/(*R,R*$_P$)-**8**.

Table 2. Catalytic hydrogenation of tiglic acid in the presence of clusters **4**-**8**.[a]

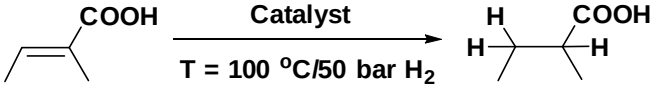

Entry	Catalyst	Conv.[b] %
1	(*S*)-**4**	51
2	(*S*,S_P)-**5**	52
3	(*S*,R_P)-**6**	49
4[c]	(*S*,R_P)-**6**	78
5	(*R*,S_P)-**7**	55
6	(*R*,R_P)-**8**	51
7[c]	(*R*,R_P)-**8**	78

[a] Reaction conditions: p(H_2) = 50 bar, T = 100 °C, t = 24 h, solvent = EtOH/toluene (1:1, 5 mL), $n_{(substrate)}/n_{(catalyst)}$ = 100.[b] Amount of substrate consumed in the catalytic experiment assessed by ^{1}H NMR spectroscopy.[c] Reaction time t = 48 h.

Clusters (*S*,R_P)-**6** and (*R*,R_P)-**8** gave quite high conversion rates (78%), when extended reaction times of 48h were employed (entries 4 and 7, Table 2). Under the same reaction conditions, [$H_4Ru_4(CO)_{12}$] did not show reasonable catalytic conversion rates (≈21%) [38]. Clusters (*S*,S_P)-**5**/(*S*,R_P)-**6** and (*R*,S_P)-**7**/(*R*,R_P)-**8** were recovered unaltered after the catalytic run in ca. 50-60% yields. After work-up, no evidence of other metal-based products was observed. Cluster (*S*)-**4** was unrecoverable at the end of the catalytic cycle - unknown/unidentifiable decomposition products were recovered instead.

However, in this study *no* enantioselectivity was observed for any of the chiral clusters which were tested as catalysts/catalyst precursors. Knowles *et al*. have proposed that in hydrogenation reactions, bidentate phosphine ligands are generally superior to monodentate ones, because their use results in greater rigidity in the molecular catalyst, which leads to higher chiral induction [39]. In clusters (*S*,S_P)-**5**/(*S*,R_P)-**6** and (*R*,S_P)-**7**/(*R*,R_P)-**8**, beside the chiral binaphthyl backbone, the stereogenic center at phosphorus is directly coordinated to a ruthenium atom in the cluster, but the effective steric bulk of this ligand is relatively small because one of the substituents on the phosphorus is a hydrogen. In cluster (*S*)-**4**, the bidentate diphosphirane ligand is coordinated to the cluster in a chelating mode, which may have been expected to lead to a better chiral induction; effective chiral induction by 1,1-[$H_4Ru_4(CO)_{10}$(P-P*)] clusters has been demonstrated previously (where P-P*= chiral diphosphine ligand) [19]. However, (*S*)-**4** gave no enantioselectivity either; one explanation is that the phosphirane ring-opening reaction that occurs in the monodentate cases also happens in this instance, generating mixed secondary/tertiary and secondary/secondary bidentate ligands, that are ineffective at chiral induction.

Whilst the above rationale is plausible, the exact reaction mechanism(s) of the cluster-based catalytic hydrogenation reaction is/are still unclear [19]. Although the isolation of (*S*,S_P)-**5**/(*S*,R_P)-**6** and (*R*,S_P)-**7**/(*R*,R_P)-**8** from the catalytic reaction is consistent with cluster-based catalysis (but does not exclude fragmentation), (*S*)-**4** also decomposes. Assuming the case of intact clusters, it should also be borne in mind that the presence of several metal centers is an inherent weakness when it comes to enantioselection in these particular systems - it is more likely that a substrate will coordinate at a ruthenium center that is remote from the coordinated chiral ligand. The effective chiral induction is thus expected to be lower than in a corresponding mononuclear complex, which illustrates the need for further research into more sophisticated cluster design.

In previous studies, an (empirical) correlation between the hydride fluxionality in clusters of the type $[H_4Ru_4(CO)_{10}(P\text{-}P^*)]$ (P-P* = chiral diphosphine ligand) and the chiral induction generated in the catalytic asymmetric hydrogenation of α-unsaturated carboxylic acids was noted. The greater the fluxionality, the lower the chiral induction [19, 22, 38], whereas clusters which were effective in this regard were found to have a very rigid hydride orientation/location. In each case, it was found that one specific hydride remained fixed under the catalytic conditions (temperature and hydrogen pressure) used in the present study [19, 22]. Thus the observed correlation also appears to hold true for the H_4Ru_4 clusters investigated in the present study; they are the most fluxional chiral tetraruthenium clusters that we have so far studied, and they give no chiral induction.

3. Conclusions

In summary, we have synthesized and characterized new tetranuclear ruthenium clusters functionalized with chiral phosphiranes, and used these to generate secondary phosphine-bound clusters, as well as a new phosphinidene-capped triruthenium cluster. All of these clusters are capable (to varying degrees) of acting as catalysts/catalyst precursors for the hydrogenation of tiglic acid; however, no chiral induction was detected in the reaction. Although it has not been possible to unambiguously determine the nature of the active catalyst in the cluster-based

systems, indirect evidence suggests that clusters (*S*,S_P)-**5**/(*S*,R_P)-**6** and (*R*,S_P)-**7**/(*R*,R_P)-**8** may be the active catalysts, or direct precursors to an active cluster catalyst.

From the present results, and based on our previous findings using various chiral phosphine derivatives of $[H_4Ru_4(CO)_{12}]$ as asymmetric hydrogenation catalysts [21, 38], it is evident that the nature of the chiral ligand is key to the enantioselectivity that is obtained. Our next intention is to design new bidentate phosphines, which will slow the hydride fluxionality by virtue of their modified steric/electronic properties.

4. Experimental

All reactions and other manipulations were carried out under a nitrogen atmosphere using standard Schlenk techniques. All solvents were dried and distilled under a nitrogen atmosphere prior to use. Infra-red spectra were recorded as solutions in 0.5 mm NaCl cells on a Nicolet Avatar 360 FT-IR spectrometer. ^{1}H and ^{31}P{^{1}H} NMR spectra were recorded on a Varian Unity 500 MHz NMR spectrometer: ^{1}H NMR shifts were referenced to Me_4Si, with ^{31}P{^{1}H} NMR shifts referenced to external H_3PO_4 (85%). The ^{31}P[^{1}H] NMR spectra of **5**-**8** have been obtained with partial ^{1}H NMR decoupling in the range of +4.0 to –30.0 ppm. The parent cluster $[(\mu\text{-}H)_4Ru_4(CO)_{12}]$ was prepared according to a literature procedure [40] and its purity assessed by thin-layer chromatographic (TLC) analysis and IR spectroscopy. The chiral phosphirane ligands [(*S*)-1-([1,1′-binaphthalen]-2-yl) phosphirane] (*S*)-**1a**, [(*R*)-1-(2′-methoxy-1,1′-binaphthyl-2-yl) phosphirane] (*R*)-**1b** and [2,2′-di(phosphiran-1-yl)-1,1′-binaphthalene] (*S*)-**1c** were prepared using the methodology outlined previously [28, 41]. Tiglic acid and (*S*)-methyl mandelate were purchased from Sigma-Aldrich. Products were separated using Merck thin-layer chromatography (TLC) plates as supplied (0.25 mm layer of Kiesel-gel 60 F254). Catalysis experiments were carried out using a 45 mL Parr autoclave with a PTFE reaction vessel.

*4.1. Synthesis of $[(\mu\text{-}H)_4Ru_4(CO)_{11}$((S)-**1a**)] (S)-**2***

$[(\mu\text{-H})_4Ru_4(CO)_{12}]$ (25 mg, 0.033 mmol) and (*S*)-**1a** (11 mg, 0.033 mmol) were dissolved in 20 mL of dichloromethane and the solution was stirred for 20 min. Under vigorous stirring, a small excess of Me_3NO (3 mg, 0.04 mmol) dissolved in dichloromethane (5 mL) was added dropwise to the yellowish cluster/ligand solution for 30 min, with an instant change of colour towards red. After 6 h the organics were removed under reduced pressure. The red solid residue was redissolved in a small quantity of dichloromethane and purified by preparative TLC (dichloromethane/petroleum ether, 1:3). Apart from traces of starting materials and one stationary brown band (decomposed material), one band was isolated from the TLC plate, extracted with dichloromethane and dried under vacuum to afford a red microcrystalline solid (R_f = 0.7). This was identified as $[(\mu\text{-H})_4Ru_4(CO)_{11}((S)\text{-}\mathbf{1a})]$ (*S*)-**2** (13 mg, 38%). ^{1}H NMR (500 MHz, $CDCl_3$): δ = 8.00 (d, *J* = 8.5 Hz, 1H), 7.93 (m, 2H), 7.85 (d, *J* = 8.3 Hz, 1H), 7.78 (m, 1H), 7.67 (app t, 1H), 7.54 (d, *J* = 6.9 Hz, 1H), 7.46 (m, 2H), 7.23 (m, 2H), 7.06 (d, *J* = 8.6 Hz, 1H), 6.95 (d, *J* = 8.1 Hz, 1H), 1.19 (m, 1H, PC_2H_4), 1.11 (m, 1H, PC_2H_4), 1.02 (m, 1H, PC_2H_4), 0.54 (m, 1H, PC_2H_4), –17.64 (d, $J_{H\text{-}H}$ = 4.6 Hz, 4H, RuHRu) ppm; ^{31}P NMR (202 MHz, $CDCl_3$): δ = –154.2 (br m, $^2J_{P\text{-}H}$ = not resolved) ppm; IR (cyclohexane): 2094 (m), 2088 (w), 2067 (vs), 2057 (vs), 2029 (vs), 2009 (vs), 1990 (m), 1969 (w) cm^{-1}; MS (FAB): *m*/*z* = 1052 $[M+Na]^+$.

*4.2. Synthesis of $[(\mu\text{-H})_4Ru_4(CO)_{11}((R)\text{-}\mathbf{1b})]$ (R)-**3***

$[(\mu\text{-H})_4Ru_4(CO)_{12}]$ (30 mg, 0.04 mmol) and (*R*)-**1b** (14 mg, 0.04 mmol) were dissolved in 20 mL of dichloromethane and the solution stirred for 20 min. Under vigorous stirring, a small excess of Me_3NO (3.6 mg, 0.048 mmol) dissolved in dichloromethane (5 mL) was added dropwise to the yellowish cluster/ligand solution for 30 min, with an instant change of colour towards red. After 6 h the organics were removed under reduced pressure. The red solid residue was redissolved in a small quantity of dichloromethane and purified by preparative TLC (dichloromethane/petroleum ether, 1:3). Apart from traces of starting materials and one stationary brown band (decomposed material), one band was isolated from the TLC plate, extracted with dichloromethane and dried under vacuum to afford a microcrystalline red solid (R_f = 0.6). This was identified as $[(\mu\text{-H})_4Ru_4(CO)_{11}((R)\text{-}\mathbf{1b})]$ (*R*)-**3** (17 mg, 42%). ^{1}H NMR (500 MHz, $CDCl_3$): δ = 8.02 (d, *J* = 9.2 Hz, 1H), 7.96 (d, *J* = 8.2 Hz, 1H), 7.86 (d, *J* = 8.0 Hz, 2H), 7.77 (m, 1H), 7.46 (m, 2H), 7.32

(m, 1H), 7.22 (m, 2H), 7.03 (d, *J* = 8.7 Hz, 1H), 6.76 (d, *J* = 8.8 Hz, 1H), 3.71 (s, 3H, OCH_3), 1.66 (m, 1H, PC_2H_4), 1.07 (m, 1H, PC_2H_4), 0.92 (m, 1H, PC_2H_4), 0.72 (m, 1H, PC_2H_4), –17.84 (s, 4H, RuHRu) ppm; ^{31}P NMR (202 MHz, $CDCl_3$): δ = –155.9 (br s) ppm; IR (cyclohexane): 2092 (m), 2086 (m), 2065 (vs), 2053 (vs), 2030 (vs), 2007 (vs), 1989 (m), 1969 (w) cm^{-1}; MS (FAB): *m*/*z* = 1081 $[M+Na]^+$.

*4.3. Synthesis of 1,1-[(μ-H)$_4$Ru$_4$(CO)$_{10}$((S)-1c)] (S)-**4***

40 mg (0.053 mmol) of [(μ-H)$_4$Ru$_4$(CO)$_{12}$] and 20 mg (0.053 mmol) of (*S*)-**1c** were dissolved in dichloromethane. A small excess of Me_3NO [6 mg, 0.08 mmol] dissolved in 5 mL of dichloromethane, containing a few drops of acetonitrile, was added dropwise over a period of 30 min to the stirred cluster/ligand solution. The initial yellow coloured solution turned deep red during the addition of Me_3NO. The reaction was monitored continuously by TLC analysis (dichloromethane/petroleum ether 1:3) and when no more parent cluster was observed (2 h), the solvent was removed under vacuum. The resulting red solid was redissolved in a small quantity of dichloromethane and separated using preparative TLC (dichloromethane/petroleum ether, 1:3). Apart from traces of starting materials, one red band was isolated from the TLC plate (R_f = 0.4), extracted with dichloromethane and dried under vacuum. This was identified as 1,1-[(μ-H)$_4$Ru$_4$(CO)$_{10}$((*S*)-**1c**)] (*S*)-**4** (16 mg, 28%). ^{1}H NMR (500 MHz, $CDCl_3$): δ = 8.00 (m, 3H), 7.92 (m, 3H), 7.83 (m, 1H), 7.73 (m, 1H), 7.50 (m, 1H), 7.23 (m, 1H), 6.80 (dd, *J* = 23.2 Hz, 8.3 Hz, 2H), 1.79 (m, 1H, PC_2H_4), 1.67 (m, 1H, PC_2H_4), 1.43 (m, 1H, PC_2H_4), 1.34 (m, 1H, PC_2H_4), 0.55 (m, 1H, PC_2H_4), 0.62 (m, 2H), 0.42 (m, 1H, PC_2H_4), –17.20 (br s, 4H, RuHRu) ppm; ^{31}P NMR (202 MHz, $CDCl_3$): δ = –135.6 (d, $^2J_{P\text{-}P}$ = 37.1 Hz), –139.2 (d, $^2J_{P\text{-}P}$ = 37.1 Hz) ppm; IR (cyclohexane): 2076 (s), 2044 (vs), 2024 (vs), 2008 (s), 1993 (w), 1987 (w), 1977 (m), 1953 (br) cm^{-1}; MS (FAB): *m*/*z* = 1082 $[M+Na]^+$. Red crystals of (*S*)-**4** were obtained by slow evaporation of dichloromethane/hexane at 4 °C.

*4.4. Synthesis of [(μ-H)$_4$Ru$_4$(CO)$_{11}$((S)-binaphthyl-P$_{(S)}$(H)Et)] (S,S$_P$)-**5** and [(μ-H)$_4$Ru$_4$(CO)$_{11}$((S)-binaphthyl-P$_{(R)}$(H)Et)] (S,R$_P$)-**6***

*4.4.1. Method A: Thermal ligand substitution at high pressure using [(μ-H)$_4$Ru$_4$(CO)$_{11}$((S)-1a)] (S)-**2***

A small laboratory autoclave (45 mL capacity), was loaded with 45 mg (0.043 mmol) of [(μ-H)$_4$Ru$_4$(CO)$_{11}$((*S*)-**1a**)] (*S*)-**2**, and dissolved in 5 mL of EtOH/toluene (1:1). The autoclave was sealed and purged three times with 10 bar of H_2 before being pressurized to 50 bar H_2. After 24 h at 100 °C, the autoclave was cooled to room temperature. The gases were carefully released and the autoclave was opened. The dark brown solution was concentrated, and the obtained solid was dissolved in 2 mL of dichloromethane and subjected to preparative TLC (dichloromethane/petroleum ether, 1:3). Apart from traces of starting materials and one stationary brown band (decomposed material), two bands were isolated from the TLC plate, extracted with dichloromethane and dried under vacuum. Two products were observed; the first product (red, R_f = 0.8) was identified as [(μ-H)$_4$Ru$_4$(CO)$_{11}$((*S*)-binaphthyl-P$_{(s)}$(H)Et)] (*S*,*S*$_P$)-**5** (8 mg, 19%). ^{1}H NMR (500 MHz, $CDCl_3$) δ = 8.15 (d, *J* = 7.1 Hz, 1H), 8.09 (d, *J* = 9.1 Hz, 1H), 7.97 (d, *J* = 8.2 Hz, 1H), 7.93 (d, *J* = 8.3 Hz, 1H), 7.67 (dd, *J* = 11.2 Hz, 8.7 Hz, 1H), 7.54 (app t, 1H), 7.39 (d, *J* = 7.8 Hz, 1H), 7.32 (m, 1H), 7.37 (m, 1H), 7.26 (app t, 2H), 7.16 (d, *J* = 8.5 Hz, 1H), 6.96 (d, *J* = 8.4 Hz, 1H), 5.23 (dd, $^1J_{P\text{-}H}$ = 381 Hz, $J_{H\text{-}H}$ = 10.7 Hz, 1H, PH), 2.13 (m, 1H, PC*H*$_2$CH$_3$), 1.85 (m, 1H, PC*H*$_2$CH$_3$), 0.86 (m, 3H, PCH$_2$C*H*$_3$), –17.64 (s, 4H, RuHRu) ppm; ^{31}P NMR (202 MHz, $CDCl_3$): δ = –11.9 (s) ppm; IR (cyclohexane): 2092 (w), 2084 (m), 2064 (m), 2051 (vs), 2030 (vs), 2012 (s), 1984 (m), 1967 (w) cm^{-1}; MS (FAB): *m*/*z* = 1035 [M+H]$^+$. The second product, (red, R_f = 0.7), was identified as [(μ-H)$_4$Ru$_4$(CO)$_{11}$((*S*)-binaphthyl-P$_{(R)}$(H)Et)] (*S*,*R*$_P$)-**6** (7 mg, 17%). ^{1}H NMR (500 MHz, $CDCl_3$): δ = 8.15 (d, *J* = 7.0 Hz, 1H), 8.07 (d, *J* = 9.1 Hz, 1H), 7.97 (d, *J* = 8.3 Hz, 1H), 7.91 (d, *J* = 8.1 Hz, 1H), 7.72 (dd, *J* = 11.5 Hz, 8.6 Hz, 1H), 7.56 (app t, 1H), 7.45 (d, *J* = 9.1 Hz, 1H), 7.35 (m, 2H), 7.27 (app t, 2H), 7.18 (d, *J* = 8.5 Hz, 1H), 6.90 (d, *J* = 8.5 Hz, 1H), 5.28 (dd, $^1J_{P\text{-}H}$ = 379 Hz, $J_{H\text{-}H}$ = 9.7 Hz, 1H, PH), 2.21 (m, 1H, PC*H*$_2$CH$_3$), 1.98 (m, 1H, PC*H*$_2$CH$_3$), 1.06 (m, 3H, PCH$_2$C*H*$_3$), –17.81 (s, 4H, RuHRu) ppm; ^{31}P NMR (202 MHz, $CDCl_3$): δ = –13.1 (s) ppm; IR (cyclohexane): 2092 (w), 2086 (m), 2063 (vs), 2057 (vs), 2052 (vs), 2030 (vs), 2007 (s), 1987 (m), 1966 (w) cm^{-1}; MS (FAB): *m*/*z* = 1035 [M+H]$^+$.

4.4.2. Method B: Thermal ligand substitution at high pressure

$[(\mu\text{-H})_4Ru_4(CO)_{12}]$ (30 mg, 0.04 mmol) and (*S*)-**1a** (13 mg, 0.04 mmol) were dissolved in 5 mL of benzene and the solution was transferred to a small autoclave (45 mL capacity). The autoclave was sealed and purged three times with 10 bar of H_2 before being pressurized to 30 bar H_2. After 4 h at 125 °C, the autoclave was cooled to room temperature. The gases were carefully released and the autoclave was opened. The isolation, purification and identification procedures of the products were identical to those described above. Yields: (S,S_P)-**5** (9 mg, 20%) and (S,R_P)-**6** (7 mg, 16%).

*4.5. Synthesis of [(μ-H)$_4$Ru$_4$(CO)$_{11}$((R)-binaphthyl-P$_{(s)}$(H)Et)] (R,S$_P$)-**7** and [(μ-H)$_4$Ru$_4$(CO)$_{11}$((R)-binaphthyl-P$_{(R)}$(H)Et)] (R,R$_P$)-**8***

*4.5.1. Method A: Thermal ligand substitution at high pressure using [(μ-H)$_4$Ru$_4$(CO)$_{11}$((R)-**1b**)] (R)-**3***

In a small laboratory autoclave (45 mL capacity), 50 mg (0.047 mmol) of $[(\mu\text{-H})_4Ru_4(CO)_{11}$((*R*)-**1b**)] (*R*)-**3** was dissolved in 5 mL of EtOH/toluene (1:1). The autoclave was sealed and purged three times with 10 bar of H_2 before being pressurized to 50 bar H_2. After 24 h at 100 °C, the autoclave was cooled to room temperature. The gases were carefully released and the autoclave was opened. The dark brown solution was concentrated and the obtained solid was dissolved in 2 mL of dichloromethane and subjected to preparative TLC (dichloromethane/petroleum ether, 1:3). Apart from traces of starting materials and one stationary brown band (decomposed material), two bands were isolated from the TLC plates, and extracted with dichloromethane and dried under vacuum. Two products were observed, the first (red, R_f = 0.5) was identified as $[(\mu\text{-H})_4Ru_4(CO)_{11}$((*R*)-binaphthyl-P$_{(s)}$(H)Et)] ($R,S_P$)-**7** (14 mg, 28%). ^{1}H NMR (500 MHz, $CDCl_3$): δ = 8.07 (d, *J* = 8.8 Hz, 1H), 8.02 (d, *J* = 9.3 Hz, 1H), 7.90 (d, *J* = 8.1 Hz, 1H), 7.86 (d, *J* = 8.3 Hz, 1H), 7.59 (m, 1H), 7.49 (app t, 1H), 7.44 (d, *J* = 9.1 Hz, 1H), 7.30 (app t, 1H), 7.25 (app t, 1H), 7.19 (m, 1H), 7.09 (d, *J* = 8.8 Hz, 1H), 6.89 (d, *J* = 8.0 Hz, 1H), 5.16 (dd, $^1J_{P\text{-}H}$ = 380 Hz, $J_{H\text{-}H}$ = 10.3 Hz, 1H, PH), 3.67 (s, 3H, OCH_3), 2.06 (m, 1H, PCH_2CH_3), 1.77 (m, 1H, PCH_2CH_3), 0.79 (m, 3H, PCH_2CH_3), –17.72 (s, 4H, RuHRu) ppm; ^{31}P NMR (202 MHz, $CDCl_3$): δ = −11.8 (s) ppm; IR (cyclohexane): 2091 (w), 2086 (m), 2061 (vs), 2052 (vs), 2030 (vs), 2012 (sh), 2005 (s), 1988 (m), 1967 (w) cm^{-1}; MS (FAB): *m*/*z* = 1083 $[M+Na]^+$.

Crystallization of (R,S_P)-**7** from a dichloromethane/hexane mixture at 4 °C yielded red crystals suitable for X-ray diffraction analysis.

The second product (red, R_f = 0.4) was identified as [(μ-H)$_4$Ru$_4$(CO)$_{11}$((R)-binaphthyl-P$_{(R)}$(H)Et)] (R,R_P)-**8** (18 mg, 36%). ^{1}H NMR (500 MHz, $CDCl_3$): δ = 8.09 (d, J = 8.3 Hz, 1H), 8.01 (d, J = 9.1 Hz, 1H), 7.92 (d, J = 8.4 Hz, 1H), 7.86 (d, J = 8.1 Hz, 1H), 7.67 (m, 1H), 7.51 (app t, 1H), 7.39 (d, J = 9.0 Hz, 1H), 7.30 (app t, 1H), 7.27 (app t, 1H), 7.22 (m, 1H), 7.13 (d, J = 8.6 Hz, 1H), 6.85 (d, J = 8.5 Hz, 1H), 5.22 (dd, $^1J_{P\text{-}H}$ = 378 Hz, $J_{H\text{-}H}$ = 9.0 Hz, 1H), 3.72 (s, 3H, OCH_3), 2.15 (m, 1H, PCH_2CH$_3$), 1.91 (m, 1H, PCH_2CH$_3$), 0.99 (m, 3H, PCH$_2$CH_3), –17.86 (s, 4H, RuHRu) ppm; ^{31}P NMR (202 MHz, $CDCl_3$): δ = –13.2 (s) ppm; IR (cyclohexane): 2092 (w), 2086 (m), 2062 (vs), 2055 (vs), 2051 (vs), 2031 (vs), 2024 (s), 2005 (s), 1988 (m), 1966 (w) cm^{-1}; MS (FAB): m/z = 1083 [M+Na]$^+$.

4.5.2. Method B: Thermal ligand substitution at high pressure

[(μ-H)$_4$Ru$_4$(CO)$_{12}$] (30 mg, 0.04 mmol) and (R)-**1b** (14 mg, 0.04 mmol) were dissolved in 6 mL of benzene and the solution was transferred to a small autoclave (45 mL capacity). The autoclave was sealed and purged three times with 10 bar of H_2 before being pressurized to 30 bar H_2. After 4 h at 125 °C, the autoclave was cooled to room temperature. The gases were carefully released and the autoclave was opened. The isolation, purification and identification procedures of the products were identical to those described above. Yields: (R,S_P)-**7** (7 mg, 16%) and (R,R_P)-**8** (6 mg, 12%).

4.6. Homogeneous catalytic experiments

In the catalysis experiments, the catalyst and substrate were loaded into the autoclave under nitrogen, followed by the addition of a degassed solvent mixture (2.5 mL of EtOH/2.5 mL of toluene). The reaction vessel was closed and purged three times with hydrogen and finally pressurized to 50 bar. The reaction mixture was continuously stirred (ca. 750 rpm) and heated up to 100 °C for 24 h. After a cooling period of approximately 45 minutes, the reaction vessel was depressurized and opened. The

reaction mixture was transferred to a 50 mL flask and concentrated under vacuum. Conversions were calculated by NMR spectroscopy. To separate the carboxylic acid product from the cluster, the reaction residue was dissolved in 10 mL of Et_2O and the carboxylic acid was extracted with sodium hydroxide solution (1M, 3 x 10 mL) and washed with Et_2O (3 x 5 mL), leaving the cluster in the organic solvent. The carboxylate was protonated with sulfuric acid and extracted with Et_2O (3 x 10 mL), washed with water (2 x 5 mL) and dried over magnesium sulfate. Evaporation of the ether under vacuum yielded the carboxylic acid quantitatively. The ether phase, from which the carboxylic acid was extracted, was concentrated under vacuum to recover the remaining cluster. The enantiomeric excess of the product was detected by derivatization of 2-methylbutyric acid with (*S*)-methyl mandelate and analysis of the resultant diastereomeric product mixture was carried out by NMR spectroscopy, as fully described by Tyrrell *et al*. [42].

4.7. Variable-temperature ^{1}H NMR spectroscopy

All deuterated solvents for NMR spectroscopy were used as received (Sigma-Aldrich). Approximately 0.5 mL of a concentrated $CDCl_3$ solution of (*S*)-**2**, (*S*)-**4**, (*S*,S_P)-**5** and (*S*,R_P)-**6** were added to an NMR tube, which was subsequently sealed under a nitrogen atmosphere. The sample tube was placed into the probe using a ceramic spinner and liquid nitrogen was used as coolant. The sample was allowed to reach equilibrium at each desired temperature for 5-10 minutes prior to shimming and data acquisition. The temperature variation ranged from 298 K to 213 K for all the samples.

4.8. X-Ray data collection and structure elucidation

The diffraction data were collected at 100 K for (*R*,S_P)-**7** and at 170 K for (*S*)-**4** and **9**, using a Nonius Kappa CCD or a Bruker AXS Kappa ApexII Duo diffractometer with Mo Kα radiation (λ = 0.71073 Å). The Denzo-Scalepack [43] or APEX2 [44] program packages were used for cell refinements and data reductions. The structure solutions were carried out using the SHELXS-97 program [45] with the WinGX graphical user interface [46]. All hydrogen atoms were placed in idealized positions.

The position of the hydrides were calculated using the XHYDEX program [47]. The crystallographic details of the reported structures ((*S*)-**4**, (*R*,S_P)-**7**, and **9**) are summarized in Table S1.

Acknowledgements

We thank the EPSRC for a Career Acceleration Fellowship EP/G005206/1 (L.J.H.) and PhD studentships (A.F. and M.A.E), and the Erasmus Mundus FFEEBB1 program office for a predoctoral fellowship (to A.F.A.).

Appendix A. Supplementary data

Supplementary data related to this article can be found at http://dx.doi.org/…..

CCDC entries no. 1531250, 1531251 and 1531252 contain the supplementary crystallographic data for compounds **4**, **7** and **9**, respectively. Copies of this information may be obtained free of charge from The Director, CCDC, 12 Union Road, Cambridge, CB2 1EZ, UK (fax: +44-1223-336033; e-mail: deposit@ccdc.cam.ac.uk or www: http://www.ccdc.cam.ac.uk).

References

[1] H.U. Blaser, F. Spindler, M. Studer, Appl. Catal., 221 (2001) 119-143.

[2] E.N. Jacobsen, A. Pfaltz, H. Yamamoto, Comprehensive Asymmetric Catalysis: Supplement 1, Springer, 2003.

[3] E.N. Jacobsen, A. Pfaltz, H. Yamamoto, Comprehensive Asymmetric Catalysis: Supplement 2, Springer, 2004.

[4] A.K. Smith, J.M. Basset, J. Mol. Catal., 2 (1977) 229-241.

[5] W.-Y. Wong, F.-L. Ting, Z. Lin, Organometallics, 22 (2003) 5100-5108.

[6] P.J. Dyson, Coordin. Chem. Rev., 248 (2004) 2443-2458.

[7] W.-Y. Wong, F.-L. Ting, Y. Guo, Z. Lin, J. Clust. Sci., 16 (2005) 185-200.

[8] G. Hogarth, S.E. Kabir, E. Nordlander, Dalton Trans., 39 (2010) 6153-6174.

[9] U. Matteoli, M. Bianchi, P. Frediani, G. Menchi, C. Botteghi, M. Marchetti, J. Organomet. Chem., 263 (1984) 243-246.

[10] M. Bianchi, G. Menchi, P. Frediani, U. Matteoli, F. Piacenti, J. Organomet. Chem., 247 (1983) 89-94.

[11] R.R. Schmidt, J. Michel, Angew. Chem. Int. Ed., 21 (1982) 72-73.

[12] G. Süss-Fink, G. Herrmann, Angew. Chem. Int. Ed., 25 (1986) 570-571.

[13] M.W. Payne, D.L. Leussing, S.G. Shore, J. Am. Chem. Soc., 109 (1987) 617-618.

[14] C. Botteghi, S. Gladiali, M. Bianchi, U. Matteoli, P. Frediani, P.G. Vergamini, E. Benedetti, J. Organomet. Chem., 140 (1977) 221-228.

[15] U. Matteoli, V. Beghetto, A. Scrivanti, J. Mol. Catal. Chem., 109 (1996) 45-50.

[16] U. Matteoli, G. Menchi, P. Frediani, M. Bianchi, F. Piacenti, J. Organomet. Chem., 285 (1985) 281-292.

[17] M. Bianchi, U. Matteoli, G. Menchi, P. Frediani, F. Piacenti, C. Botteghi, J. Organomet. Chem., 195 (1980) 337-346.

[18] A. Salvini, P. Frediani, M. Bianchi, F. Piacenti, L. Pistolesi, L. Rosi, J. Organomet. Chem., 582 (1999) 218-228.

[19] P. Homanen, R. Persson, M. Haukka, T.A. Pakkanen, E. Nordlander, Organometallics, 19 (2000) 5568-5574.

[20] M.J. Stchedroff, V. Moberg, E. Rodriguez, A.E. Aliev, J. Bottcher, J.W. Steed, E. Nordlander, M. Monari, A.J. Deeming, Inorg. Chim. Acta, 359 (2006) 926-937.

[21] V. Moberg, M. Haukka, I.O. Koshevoy, R. Ortiz, E. Nordlander, Organometallics, 26 (2007) 4090-4093.

[22] V. Moberg, R. Duquesne, S. Contaldi, O. Röhrs, J. Nachtigall, L. Damoense, A.T. Hutton, M. Green, M. Monari, D. Santelia, M. Haukka, E. Nordlander, Chem. Eur. J., 18 (2012) 12458-12478.

[23] C. Claver, E. Fernandez, A. Gillon, K. Heslop, D.J. Hyett, A. Martorell, A.G. Orpen, P.G. Pringle, Chem. Commun., (2000) 961-962.

[24] M.T. Reetz, G. Mehler, Angew. Chem. Int. Ed., 39 (2000) 3889-3890.

[25] M. van den Berg, A.J. Minnaard, E.P. Schudde, J. van Esch, A.H.M. de Vries, J.G. de Vries, B.L. Feringa, J. Am. Chem. Soc., 122 (2000) 11539-11540.

[26] E.P.A. Couzijn, A.W. Ehlers, J.C. Slootweg, M. Schakel, S. Krill, M. Lutz, A.L. Spek, K. Lammertsma, Chem. Eur. J., 14 (2008) 1499-1507.

[27] A. Marinetti, F. Mathey, L. Ricard, Organometallics, 12 (1993) 1207-1212.

[28] A. Ficks, I. Martinez-Botella, B. Stewart, R.W. Harrington, W. Clegg, L.J. Higham, Chem Commun, 47 (2011) 8274-8276.

[29] A. Ficks, W. Clegg, R.W. Harrington, L.J. Higham, Organometallics, 33 (2014) 6319-6329.

[30] M. Gabriela Ballinas-López, E.V. García-Báez, M.a.J. Rosales-Hoz, Polyhedron, 22 (2003) 3403-3411.

[31] R.D. Wilson, S.M. Wu, R.A. Love, R. Bau, Inorg. Chem., 17 (1978) 1271-1280.

[32] F. Mathey, Chem. Rev., 90 (1990) 997-1025.

[33] A.U. Härkönen, M. Ahlgrén, T.A. Pakkanen, J. Pursiainen, J. Organomet. Chem., 530 (1997) 191-197.

[34] T.M. Räsänen, S. Jääskeläinen, T.A. Pakkanen, J. Organomet. Chem., 553 (1998) 453-461.

[35] C.J. Adams, M.I. Bruce, E. Horn, B.W. Skelton, E.R.T. Tiekink, A.H. White, J. Chem. Soc. Dalton Trans., (1993) 3299-3312.

[36] A.F. Abdel-Magied, M.H. Majeed, A. Ficks, A.K. Singh, W. Clegg, M. Haukka, M. Monari, E. Nordlander, L.J. Higham, unpublished results.

[37] F. Iwasaki, M.J. Mays, P.R. Raithby, P.L. Taylor, P.J. Wheatley, J. Organomet. Chem., 213 (1981) 185-206.

[38] V. Moberg, P. Homanen, S. Selva, R. Persson, M. Haukka, T.A. Pakkanen, M. Monari, E. Nordlander, Dalton Trans., (2006) 279-288.

[39] W.S. Knowles, M.J. Sabacky, B.D. Vineyard, D.J. Weinkauff, J. Am. Chem. Soc., 97 (1975) 2567-2568.

[40] S.A.R. Knox, J.W. Koepke, M.A. Andrews, H.D. Kaesz, J. Am. Chem. Soc., 97 (1975) 3942-3947.

[41] R.M. Hiney, L.J. Higham, H. Müller-Bunz, D.G. Gilheany, Angew. Chem. Int. Ed., 45 (2006) 7248-7251.

[42] E. Tyrrell, M.W.H. Tsang, G.A. Skinner, J. Fawcett, Tetrahedron, 52 (1996) 9841-9852.

[43] Z. Otwinowski, W. Minor, Processing of X-ray diffraction data collected in oscillation mode, in: Charles W. Carter, Jr. (Ed.) Methods in Enzymology, Academic Press, 1997, pp. 307-326.

[44] Bruker (2009). APEX2, GIS, SADABS and SAINT. Bruker AXS Inc., Madison, Wisconsin, USA.

[45] G. Sheldrick, Acta Cryst., 64 (2008) 112-122.

[46] L.J. Farrugia, J. Appl. Cryst., 32 (1999) 837-838.

[47] A.G. Orpen, J. Chem. Soc. Dalton Trans., (1980) 2509-2516.

Highlights

- Tetranuclear tetrahydrido ruthenium carbonyl clusters containing chiral phosphiranes were synthesized.
- Hydrogenation of the rings in the coordinated phosphirane ligands led to formation of secondary phosphine ligands with an additional sterogenic center at the phosphorus.
- The clusters showed good activity in the hydrogenation of tiglic acid (*trans*-2-methyl-2-butenoic acid).